SCIENTIFIC REPORTS

OPEN

SUBJECT AREAS:
CHEMICAL BIOLOGY
BIOPHYSICAL CHEMISTRY

Received
9 June 2014

Accepted
16 July 2014

Published
4 August 2014

Correspondence and requests for materials should be addressed to P.D.M. (pdmascio@iq.usp.br) or E.J.H.B. (ebechara@iq.usp.br)

Excited singlet molecular O_2 ($^1\Delta_g$) is generated enzymatically from excited carbonyls in the dark

Camila M. Mano[1], Fernanda M. Prado[1], Júlio Massari[1], Graziella E. Ronsein[1], Glaucia R. Martinez[2], Sayuri Miyamoto[1], Jean Cadet[3], Helmut Sies[4], Marisa H. G. Medeiros[1], Etelvino J. H. Bechara[1,5] & Paolo Di Mascio[1]

[1]Departamento de Bioquímica, Instituto de Química, Universidade de São Paulo, CEP 05513-970, CP 26077, São Paulo, SP, Brazil, [2]Departamento de Bioquímica e Biologia Molecular, Setor de Ciências Biológicas, Universidade Federal do Paraná, Curitiba, PR, Brazil, [3]Institut Nanosciences et Cryogénie, CEA/Grenoble, F-38054 Grenoble Cedex 9, France, [4]Institute of Biochemistry and Molecular Biology I, and Leibniz Research Institute for Environmental Medicine, Heinrich-Heine-Universität Düsseldorf, Düsseldorf, Germany, [5]Departamento de Ciências Exatas e da Terra, Instituto de Ciências Ambientais, Químicas e Farmacêuticas, Universidade Federal de São Paulo, SP, Brazil.

In mammalian tissues, ultraweak chemiluminescence arising from biomolecule oxidation has been attributed to the radiative deactivation of singlet molecular oxygen [O_2 ($^1\Delta_g$)] and electronically excited triplet carbonyl products involving dioxetane intermediates. Herein, we describe evidence of the generation of O_2 ($^1\Delta_g$) in aqueous solution via energy transfer from excited triplet acetone. This involves thermolysis of 3,3,4,4-tetramethyl-1,2-dioxetane, a chemical source, and horseradish peroxidase-catalyzed oxidation of 2-methylpropanal, as an enzymatic source. Both sources of excited carbonyls showed characteristic light emission at 1,270 nm, directly indicative of the monomolecular decay of O_2 ($^1\Delta_g$). Indirect analysis of O_2 ($^1\Delta_g$) by electron paramagnetic resonance using the chemical trap 2,2,6,6-tetramethylpiperidine showed the formation of 2,2,6,6-tetramethylpiperidine-1-oxyl. Using [^{18}O]-labeled triplet, ground state molecular oxygen [$^{18}O_2$ ($^3\Sigma_g^-$)], chemical trapping of $^{18}O_2$ ($^1\Delta_g$) with disodium salt of anthracene-9,10-diyldiethane-2,1-diyl disulfate yielding the corresponding double-[^{18}O]-labeled 9,10-endoperoxide, was detected through mass spectrometry. This corroborates formation of O_2 ($^1\Delta_g$). Altogether, photoemission and chemical trapping studies clearly demonstrate that chemically and enzymatically nascent excited carbonyl generates $^{18}O_2$ ($^1\Delta_g$) by triplet-triplet energy transfer to ground state oxygen O_2 ($^3\Sigma_g^-$), and supports the long formulated hypothesis of O_2 ($^1\Delta_g$) involvement in physiological and pathophysiological events that might take place in tissues in the absence of light.

The generation of excited triplet carbonyls and of singlet molecular oxygen, O_2 ($^1\Delta_g$), has long been reported to occur in various biological processes, based on the observation of low-level (also called ultraweak) chemiluminescence (CL)[1–11].

Triplet-excited carbonyl species can be generated by photoexcitation of carbonyl compounds. Importantly, electronically excited carbonyls can also be generated by chemiexcitation and undergo further typical photochemical processes, i.e. without photoexcitation, which consequently was independently called by G. Cilento (University of São Paulo)[10] and by E. H. White (Johns Hopkins University) as "*photochemistry in the dark*"[11]. Some examples of such "dark" reactions are the dismutation of alkoxyl radicals[12], thermal decomposition of 1,2-dioxetanes[13,14], thermolysis of oxetanes (reverse [2+2] Paternò-Büchi reaction)[15], and dismutation of alkyl peroxyl radicals, known as the Russell reaction[16,17]. The quantum yield of excited triplet carbonyl generation may vary from 0.1% up to 60% in these reactions[18]. Of potential biological interest are triplet carbonyls arising from the annihilation of oxyradical intermediates during lipid peroxidation[6,18–21].

Enzyme-catalyzed peroxidation can also yield excited triplet carbonyls, as in the case of aerobic oxidation of 2-methylpropanal (isobutyraldehyde or isobutanal, IBAL) catalyzed by horseradish peroxidase (HRP), which gives rise to formic acid and triplet acetone[22]. This reaction is thought to occur by HRP-catalyzed addition of molecular oxygen to the α-carbon of IBAL, yielding a 1,2-dioxetane intermediate whose homolysis renders acetone in the triplet state[22–24]. Accordingly, the chemiluminescence spectrum matches the phosphorescence spectrum of triplet acetone ($\lambda_{max} \sim 430$ nm). In addition, *iso*-propanol and pinacol (2,3-dihydroxypropane) ultimately formed by

hydrogen abstraction from the carbohydrate portion of HRP by triplet acetone were found in the spent reaction mixtures, thus a process that can be here classified as a source of "photo" chemical products, although formed in the dark.

The fact that the excitation energy of acetone to its triplet state is about 335 kJ.mol^{-1} [12] whereas that of O_2 ($^1\Delta_g$) is 94.2 kJ.mol^{-1} [25,26] makes the triplet-triplet energy transfer process thermodynamically viable. Briviba *et al.*[27] detected monomol light emission of O_2 ($^1\Delta_g$) at 1,270 nm in CCl_4 during the thermal decomposition of 3-hydroxymethyl-3,4,4-trimethyl-1,2-dioxetane.

Singlet molecular oxygen exhibits a pair of electrons whose opposite spins in the highest occupied molecular orbital gives O_2 ($^1\Delta_g$) dienophilic properties, which explains its significant reactivity toward electron-rich organic molecules, particularly with those exhibiting conjugated double bonds[28], leading to the formation of allylic hydroperoxides, dioxetanes or endoperoxides[2,5,17,29,30]. Singlet molecular oxygen has been shown to be generated in biological systems. As possible biological sources of O_2 ($^1\Delta_g$), one can cite (i) enzymatic processes catalyzed by peroxidases or oxygenases; (ii) several reactions that take place in cells, such as annihilation of lipid peroxyl radicals (Russell reaction)[16,17,30,31]; (iii) ozone oxidation of amino acids, peptides and proteins[32]; (iv) reactions of hydrogen peroxide with hypochlorite or peroxynitrite[33–35]; (v) thermolysis of endoperoxides[36–45]; (vi) *in vitro* photodynamic processes involving type II photosensitization reactions by suitable dyes[46–49]; (vii) UV irradiation of aromatic amino acids in proteins and immunoglobulins[5,50]; and (viii) metal-induced decomposition of a thymine hydroperoxide[51]. Production of O_2 ($^1\Delta_g$) during phagocytosis in polymorphonuclear leukocytes has also been described[52–54] and observed in photodynamic therapy, where the production of this reactive oxygen species (ROS) has been demonstrated using different photosensitizers, including methylene blue, eosin and rose bengal[46] or dye-containing nanoparticles[47,48]. Some endogenous photosensitizers may also lead to the generation of O_2 ($^1\Delta_g$) upon exposure to UVA radiation[5,55]. Photodynamic therapy has been applied successfully in both antimicrobial and antitumor treatments[46–49], including inactivation of viruses in human plasma[56].

Thus, there is a potential mechanistic crosstalk between O_2 ($^1\Delta_g$) and triplet carbonyl in biological environments where both excited species can be produced, either by alkoxyl and alkylperoxyl radical dismutation or by triplet-triplet energy transfer from excited carbonyls. Hence, several hypotheses, such as the production of triplet carbonyls from O_2 ($^1\Delta_g$)-driven peroxidation of polyunsaturated fatty acids, have been proposed and demonstrated experimentally, although triplet carbonyl products have been detected in only a few systems[21].

This investigation addresses the question whether electronically excited O_2 ($^1\Delta_g$) can unequivocally be produced by energy transfer from excited triplet acetone to triplet molecular oxygen O_2 ($^3\Sigma_g^-$) dissolved in aqueous solution. We used the thermolysis of 3,3,4,4-tetramethyl-1,2-dioxetane (TMD)[57,58] and the HRP/IBAL/O_2 system[22] as chemical and enzymatic sources of triplet acetone, respectively[12]. The generation of O_2 ($^1\Delta_g$) was monitored by direct spectroscopic detection and characterization of O_2 ($^1\Delta_g$) monomol light emission in the near-infrared region at 1,270 nm. Singlet molecular oxygen was also detected indirectly by electron paramagnetic resonance spectroscopy (EPR) of 2,2,6,6-tetramethylpiperidine-1-oxyl (TEMPO) formed by the reaction of the spin trap 2,2,6,6-tetramethylpiperidine (TEMP) with O_2 ($^1\Delta_g$). Further, the reaction mechanism was investigated by tracing the energy transfer from triplet excited ketone species to [^{18}O]-labeled triplet molecular oxygen [$^{18}O_2$ ($^3\Sigma_g^-$)] through the detection of [^{18}O]-labeled O_2 ($^1\Delta_g$) [$^{18}O_2$ ($^1\Delta_g$)]. Chemical trapping experiments of $^{16}O_2$ ($^1\Delta_g$) and $^{18}O_2$ ($^1\Delta_g$) were performed using the anthracene-9,10-diyldiethane-2,1-diyl disulfate disodium salt (EAS) trap by monitoring the corresponding endoperoxide (EAS^{x}O^{x}O, x = 16 or 18) with high-performance liquid chromatography coupled to electrospray ionization tandem mass spectrometry (HPLC-ESI-MS/MS).

Results

Characterization of singlet molecular oxygen generated by energy transfer from triplet acetone to triplet molecular oxygen by CL measurements. Chemiluminescence produced by a chemical reaction provides useful information about the excited species being generated. Here, the production of O_2 ($^1\Delta_g$) in response to the collision of excited triplet acetone with ground state molecular oxygen was investigated by monitoring the near infrared (NIR) light emission at 1,270 nm, which corresponds to the singlet delta state monomolecular light emission decay of oxygen ($^1\Delta_g \rightarrow {}^3\Sigma_g^-$) (Equation 1)[2,59,60]. The measurement of ultra-weak light emission or low level CL originating from this radioactive transition is an important method for the detection and characterization of O_2 ($^1\Delta_g$).

$$O_2(^1\Delta_g) \rightarrow O_2\left(^3\Sigma_g^-\right) + h\upsilon \ (\lambda = 1{,}270 \text{ nm}) \qquad (1)$$

The CL arising from the thermal decomposition of 10 mM TMD at 70°C in air-equilibrated CCl_4 or acetonitrile (Fig. 1A(b) and 1A(a), respectively) was recorded in the UV-visible region. The CL spectrum of 10 mM TMD in CCl_4 shows a peak at 430 nm (Fig. 1B), which was assigned to the triplet excited acetone[14]. Fig. 1C and 1D depict the time course of monomol light emission of O_2 ($^1\Delta_g$) at λ = 1,270 nm and the NIR spectrum of O_2 ($^1\Delta_g$), respectively. Since the lifetime of O_2 ($^1\Delta_g$) in acetonitrile is much lower than in CCl_4 (5.0–8.0 $\times$ 10^{-5} s and 0.02–0.08 s, respectively), the TMD/O_2 ($^3\Sigma_g^-$) NIR light emission in acetonitrile was very low under similar experimental conditions[61,62]. For comparison, the time course and spectrum of NIR light emission were recorded during the thermolysis of 1,4-dimethylnaphthalene-1,4-endoperoxide ($DMNO_2$)[60] in methanol (Fig. 1E and 1F).

The rate of triplet ketone produced by TMD concentrations ranging from 2 to 10 mM in CCl_4 was estimated to be 4.89 $\pm$ 0.98 nM min^{-1}. The molecular oxygen concentration available in the solvent induces a saturation effect of O_2 ($^1\Delta_g$) steady-state concentration. Briviba *et al.*[27] estimated the yield of O_2 ($^1\Delta_g$) produced by an analogue of TMD, 3,3,4,-tetramethyl-4-hydroxy-1,2-dioxetane to be 0.2%.

Since the concentration of O_2 in solution can limit the generation of O_2 ($^1\Delta_g$) by TMD thermolysis, additional luminescence experiments were performed using CCl_4. Ten minutes after starting the reaction, pure O_2 was purged inside the cuvette in an attempt to enhance O_2 ($^1\Delta_g$) generation (Fig. 2). As expected, the influx of molecular O_2 into the system decreased the intensity of UV-visible light (Fig. 2A) due to energy transfer of the generated triplet acetone to molecular oxygen, although a slight decrease in NIR monomol light emission of O_2 ($^1\Delta_g$) was observed (Fig. 2B). In this respect, we note that, although triplet molecular oxygen is known to be a triplet carbonyl suppressor[18], McGarvey *et al.*[61] reported an inverse correlation between molecular oxygen quenching of different triplet naphthalenes in benzene and the generation of O_2 ($^1\Delta_g$). This finding was then correlated to structural differences in naphthalene, and not to changes in O_2 concentration.

Since the sorbate anion was proposed as a probe for testing the presence or intermediacy and roles of triplet species in biological systems[18], the quenching effect of sorbate on TMD-generated triplet acetone luminescence was also examined (Supplementary Fig. 1).

Although 0.5 mM sorbate was able to quench ~25% of the triplet acetone chemiluminescence in CCl_4 (Supplementary Fig. 1A), the NIR light emission generated by O_2 ($^1\Delta_g$) did not change significantly (Supplementary Fig. 1B).

Triplet acetone is also produced by O_2-mediated oxidation of IBAL by molecular oxygen, catalyzed by HRP (Fig. 3). The total

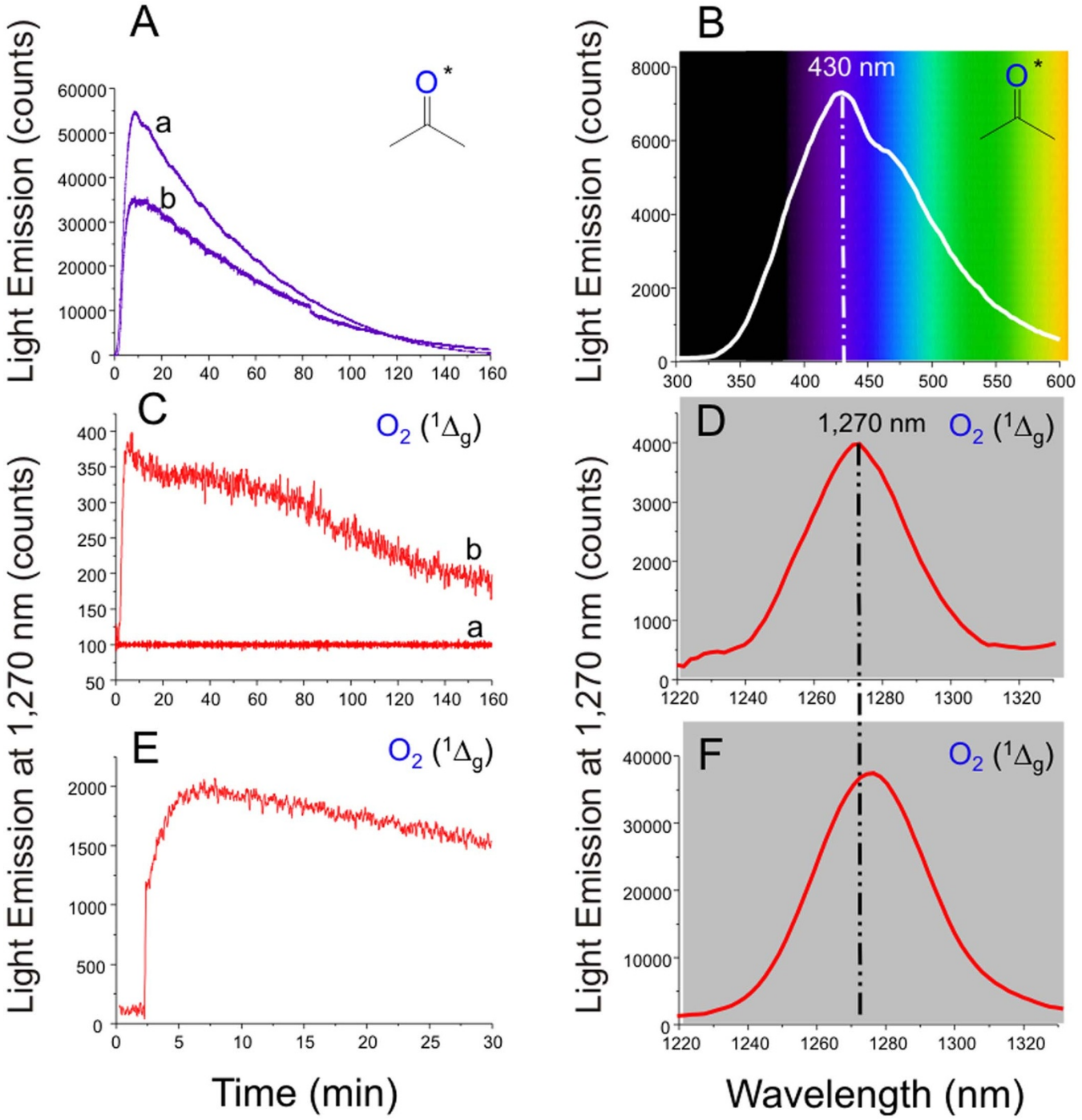

Figure 1 | **Chemiluminescence studies of TMD in organic solvents.** TMD (10 mM) was incubated in air-equilibrated organic solvents at 70°C. (A) Time course of total UV-visible light emission of TMD in acetonitrile (line a) and in CCl_4 (line b); (B) The chemiluminescence spectrum matches the phosphorescence spectrum of TMD-generated triplet excited acetone[20] in CCl_4; (C) NIR light emission of O_2 ($^1\Delta_g$) at 1,270 nm during the thermolysis of TMD in CCl_4 (line b) and in acetonitrile (line a); (D) O_2 ($^1\Delta_g$) spectrum, corresponding to the monomol light emission recorded during incubation of TMD in CCl_4; and (E and F) thermodissociation of 10 mM $DMNO_2$ in methanol, as a control, which generated O_2 ($^1\Delta_g$) monomol light emission at 1,270 nm and the NIR spectrum of released O_2 ($^1\Delta_g$), respectively.

chemiluminescence was recorded in D_2O at pD 7.4 in the presence of 5 μM HRP and 10 mM IBAL (Fig. 3A). Low-level O_2 ($^1\Delta_g$) NIR light emission was also detected at 1,270 nm under similar experimental conditions (Fig. 3B).

Singlet Molecular Oxygen Spectrum in the Near-Infrared Region. The generation of O_2 ($^1\Delta_g$) by the thermal cleavage of TMD was also confirmed by recording the spectrum of the light emitted in the near-infrared (NIR) region (Fig. 1D). For comparison, the spectrum of O_2 ($^1\Delta_g$) generated by thermolysis of $DMNO_2$[60] was also recorded (Fig. 1F). Both spectra showed an emission band with maximum intensity at 1,270 nm, characteristic of the monomolecular decay of singlet oxygen delta state. Additional proof that the light emitted in the TMD reaction corresponds to O_2 ($^1\Delta_g$) was obtained by testing the effect of solvents. The intensity of light emitted in the reaction performed in CCl_4 was higher than in acetonitrile, which is consistent

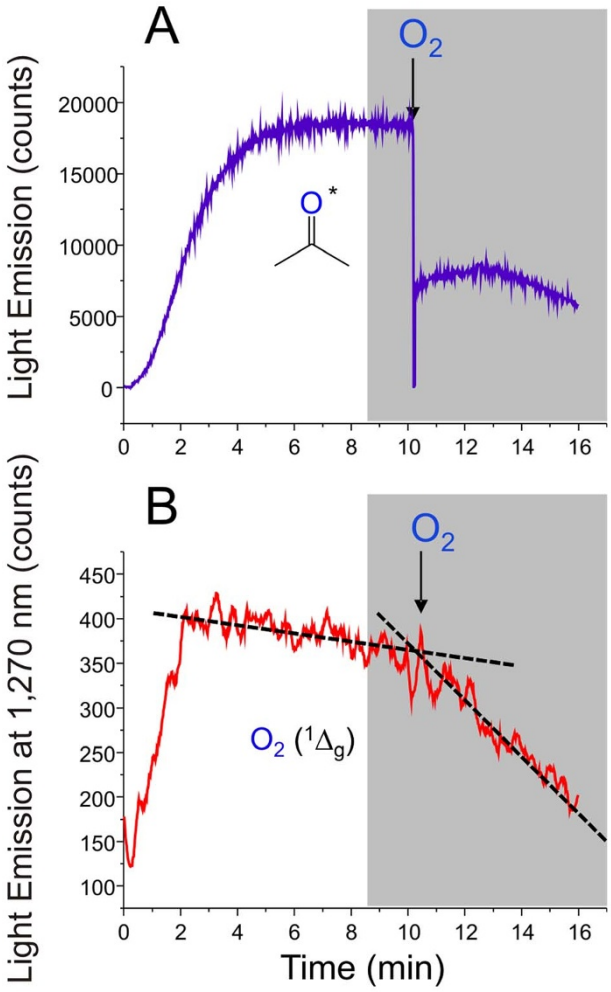

Figure 2 | Effect of pure O_2 purging on the chemiluminescence intensity elicited by TMD. (A) UV-visible light emission time course of triplet excited acetone during the thermolysis of 5 mM TMD in CCl_4 at 70°C, and (B) Monomol light emission of O_2 ($^1\Delta_g$) recorded during the decomposition of 5 mM TMD in CCl_4 at 70°C. The arrow in both graphs indicates the time elapsed in O_2 purging.

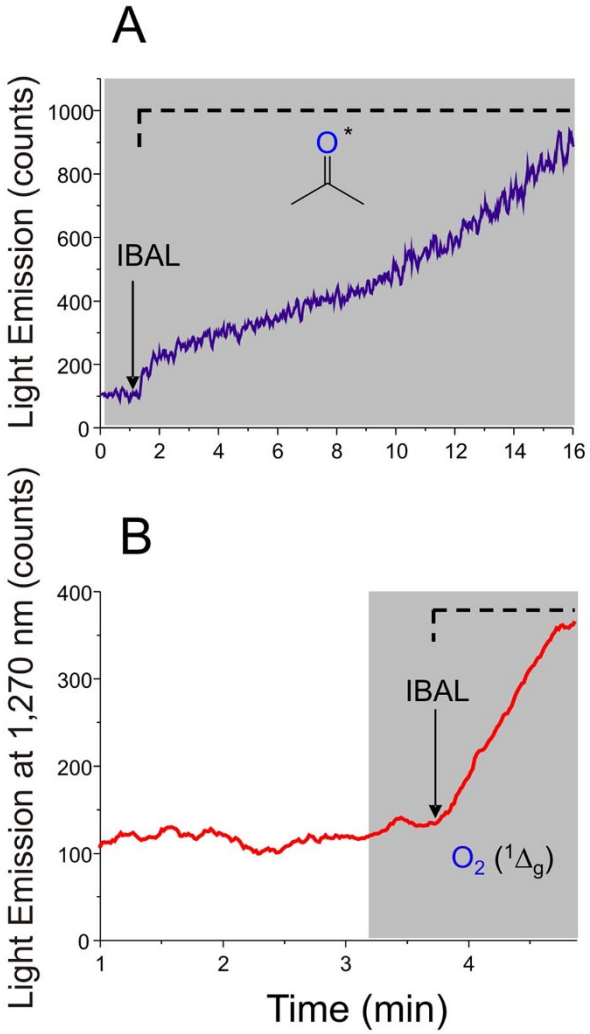

Figure 3 | Chemiluminescence studies of O_2-mediated oxidation of IBAL catalyzed by HRP. (A) Total UV-visible light emission of triplet excited acetone in deuterated phosphate buffer (pD 7.4), and (B) NIR light emission of O_2 ($^1\Delta_g$) at 1,270 nm after injection of 10 mM IBAL in a solution of 5 μM HRP in D_2O, pD 7.4 at 37°C.

with the longer lifetime of O_2 ($^1\Delta_g$) in CCl_4[62]. The quenching effect of lycopene[63] on the NIR chemiluminescent reaction of TMD thermolysis was also observed (data not shown).

Detection of O_2 ($^1\Delta_g$) by EPR. Indirect analysis of O_2 ($^1\Delta_g$) in D_2O by electron paramagnetic resonance was performed using 2,2,6,6-tetramethylpiperidine (TEMP) as the spin trap (Supplementary Fig. 2). The lifetime of O_2 ($^1\Delta_g$) in D_2O is similar to that observed in acetonitrile (5.0–6.5 × 10^{-5} s)[62]. The EPR spectrum depicted in Supplementary Fig. 2A (line a) shows a triplet signal (a_N = 1.60 mT, g-shift = −0.5) obtained upon incubation of 30 mM TEMP with 4 mM TMD in normally aerated D_2O. The pre-addition of 0.4 μM commercial standard 2,2,6,6-tetramethylpiperidine-1-oxyl (TEMPO) to the reaction mixture intensified the EPR signal significantly, thus suggesting the generation of O_2 ($^1\Delta_g$)[64] (line b).

EPR experiments using TEMP were also conducted with the HRP/IBAL system, as depicted in Supplementary Fig. 2B. The EPR spin-trapping signal obtained also overlaps the TEMPO signal, showing the same coupling constants. This finding provides further evidence of the generation of O_2 ($^1\Delta_g$) by the HRP-treated aldehyde[65].

When the reaction of TMD was conducted in the presence of 30 mM TEMP and 32 mM sorbate, no significant decrease in TEMPO was observed (data not shown). Although sorbate can reportedly suppress triplet acetone generated from TMD[18], diene quenching was unable to compete actively with the excitation of oxygen in the presence of TEMP.

When 20 μM HRP and 50 mM IBAL were incubated with 8 mM sorbate, the EPR signal of TEMPO was suppressed (Supplementary Fig. 2B, line e).

Detection of [^{18}O]-Labeled Singlet Molecular Oxygen in the Chemical and Enzymatic Reactions. To better characterize the mechanism involved in the generation of O_2 ($^1\Delta_g$) by the thermolysis of TMD or HRP-catalyzed aerobic oxidation of IBAL, [^{18}O]-labeled O_2 ($^3\Sigma_g^-$) was used as a triplet energy acceptor. The generated [^{18}O]-labeled O_2 ($^1\Delta_g$) was trapped with the anthracene derivative, EAS (Fig. 4)[5,30]. The corresponding endoperoxides (EAS^{x}O^{x}O, x = 16 or 18) were detected by HPLC-ESI-MS/MS.

In the dark, energy transfer from triplet ketone to $^{16}O_2$ or [^{18}O]-labeled molecular oxygen led to a mixture of mainly two anthracene endoperoxide derivatives, namely, the fully labeled 9,10-endoperoxide (EAS $^{18}O^{18}O$) and the related unlabeled endoperoxide (EAS $^{16}O^{16}O$), plus a small amount of partially labeled endoperoxide (EAS$^{18}O^{16}O$).

Figures 5 and 6 and Supplementary Fig. 3 to 7 show the typical chromatograms for EAS^{x}O^{x}O analysis with UV and MS/MS detec-

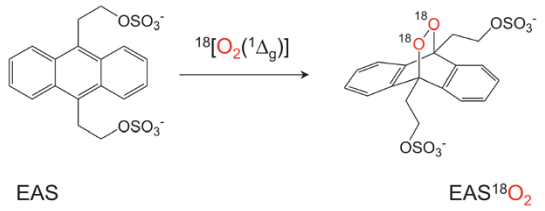

Figure 4 | Chemical trapping of [^{18}O]-labeled O_2 ($^1\Delta_g$) [$^{18}O_2$ ($^1\Delta_g$)] with disodium salt of anthracene-9,10-diyldiethane-2,1-diyl disulfate (EAS) yielding the corresponding double-[^{18}O]-labeled 9,10-endoperoxide ($EAS^{18}O_2$).

tion. Analysis of the products by UV absorption at 210 nm showed two peaks corresponding to the endoperoxides $EAS^{18}O^{18}O$ and $EAS^{16}O^{16}O$ and to EAS at the time windows 7.2 to 7.9 min and 9.2 to 12.2 min, respectively, for the TMD (Fig. 5A and Supplementary Fig. 3A) and HRP/IBAL systems (Fig. 6A and Supplementary Fig. 4A and 5A). The tandem mass spectrometry detection of $EAS^{18}O^{18}O$ (*m/z* 230→212) and $EAS^{16}O^{16}O$ (*m/z* 228→212) was performed by the Selected Reaction Monitoring (SRM) mode. SRM detection based on the fragmentation of precursor ions at *m/z* 230 (Fig. 5B and 6B) and 228 (Fig. 5C and 6C), which generated the product ion at *m/z* 212, shows the presence of $EAS^{18}O^{18}O$ and $EAS^{16}O^{16}O$, respectively. The identity of the precursor ions was confirmed based on an analysis of the mass spectra of product ions derived from each of the endoperoxides (Fig. 5E and 5F,and Fig. 6E and 6F).

Energy transfer from excited triplet acetone generated by thermal cleavage of TMD. The thermolysis of 10 mM TMD in deuterated phosphate buffer (pD 7.4) performed in an $^{16}O_2$ or $^{18}O_2$ atmosphere resulted in the generation of the corresponding EAS 9,10-endoperoxides containing the ^{18}O or ^{16}O isotope (EAS^xO^xO) (Fig. 5 and Supplementary Fig. 3).

Formation of endoperoxides, which was confirmed by HPLC-ESI-MS/MS analysis, occurred through the mass transition of *m/z* 230 →212 to $EAS^{18}O^{18}O$ and *m/z* 228 →212 to $EAS^{16}O^{16}O$ (Fig. 5B and 5C and Supplementary Fig. 3B and 3C). In the presence of [^{18}O]-labeled O_2, the amount of $EAS^{18}O^{18}O$ (Fig. 5B) was ten-fold greater than that of $EAS^{16}O^{16}O$ (Fig. 5C). The $EAS^{18}O_2$ endoperoxide formed in the presence of the triplet acetone chemical generator system shows an intense $[M\text{-}2H]^{2-}$ ion at *m/z* 230 corresponding to a molecular weight of 462 (Fig. 5D). This strongly attests to the incorporation of two [^{18}O]-labeled oxygen atoms into the anthracene derivative molecule. This finding also confirms that O_2 ($^1\Delta_g$) is produced by energy transfer from TMD-generated triplet acetone, and not through direct oxygen atom transfer from the 1,2-dioxetane, which lacks ^{18}O in its molecular structure. Important to note is the fact that the amount of $EAS^{18}O_2$ formed in the experiment reached a level of 90%[38].

Energy transfer from enzymatically generated excited triplet acetone. The generation of O_2 ($^1\Delta_g$) by energy transfer from HRP-catalyzed production of excited triplet acetone from IBAL oxidation was monitored using water-soluble EAS, which can react with O_2 ($^1\Delta_g$), yielding $EASO_2$ as the specific oxidation product (Fig. 4). To this end, EAS was incubated at 37°C with HRP and IBAL in an $^{16}O_2$

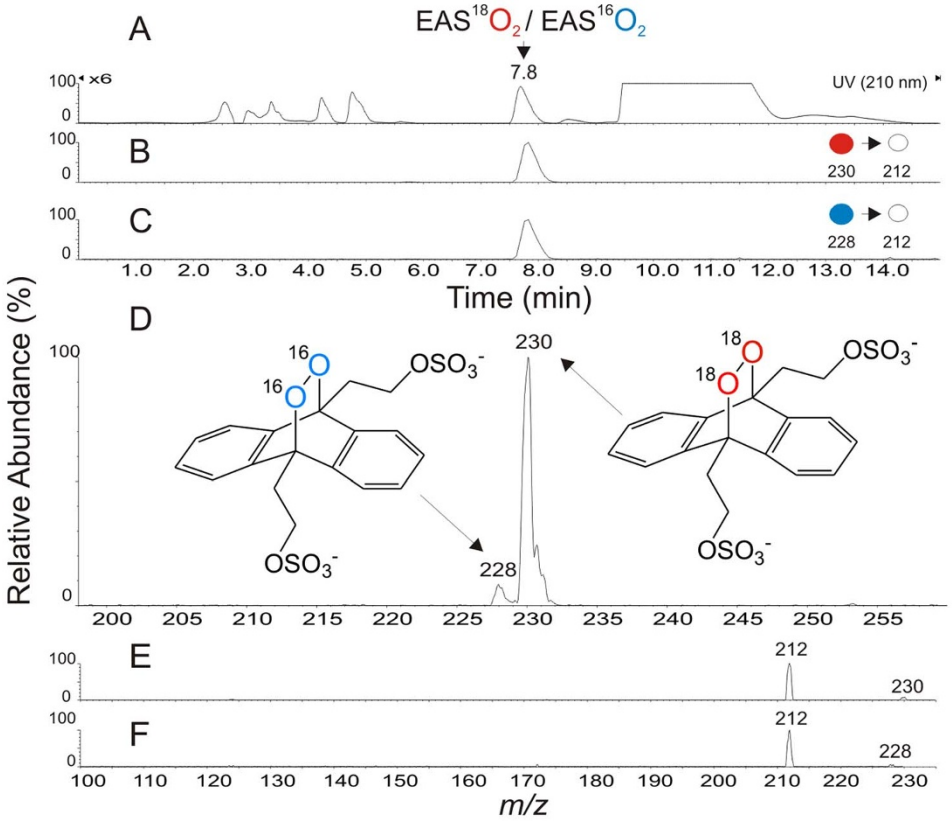

Figure 5 | EAS chemical quenching studies of O_2 ($^1\Delta_g$) produced during thermal cleavage of TMD in the presence of [^{18}O]-labeled molecular oxygen. HPLC-ESI-MS/MS analysis of 8 mM EAS incubated with 8 mM TMD for 2 h at 70°C in deuterated phosphate buffer (pD 7.4). (A) UV chromatogram at 210 nm. $EASO_2$ endoperoxides containing ^{16}O or ^{18}O eluted at 7.8 min. (B) SRM chromatogram of $EAS^{18}O^{18}O$ (*m/z* 230→212) with a determined area integration of 118,754 (A.U.). (C) SRM chromatogram of $EAS^{16}O^{16}O$ (*m/z* 228→212) with area integration of 11,882 (A.U.). (D) Full mass spectrum obtained from peak at 7.8 min within the mass range of 200-255 *m/z*. (E) Product ion spectrum from precursor ion at *m/z* 230, and (F) Product ion spectrum from precursor ion at *m/z* 228.

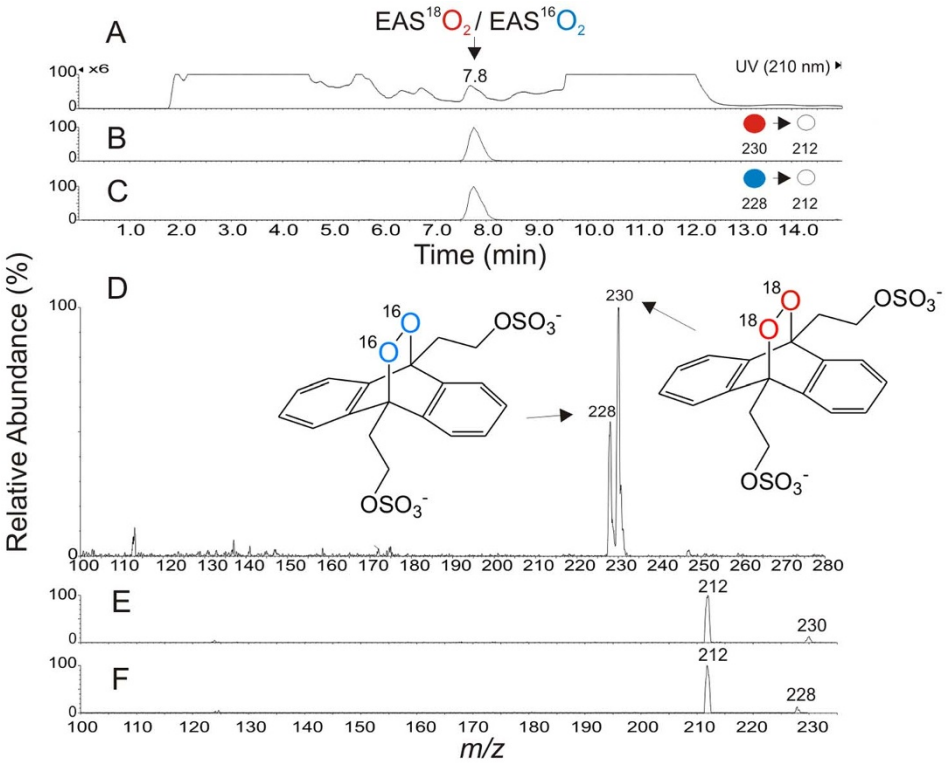

Figure 6 | EAS chemical trapping of O_2 ($^1\Delta_g$) generated by the HRP-catalyzed oxidation of IBAL in the presence of [^{18}O]-labeled molecular oxygen. HPLC-ESI-MS/MS analysis of 8 mM EAS upon incubation for 24 h with 5 μM HRP and 50 mM IBAL at 37°C in deuterated phosphate buffer (pD 7.4). (A) UV chromatogram at 210 nm. Endoperoxides EAS^{16}O^{16}O and EAS^{18}O^{18}O eluted at 7.8 min. (B) SRM chromatogram of EAS^{18}O^{18}O (*m/z* 230→212). (C) SRM chromatogram of EAS^{16}O^{16}O (*m/z* 228→212). (D) Full mass spectrum obtained from peak at 7.8 min within mass range of 100–280 *m/z*. (E) Product ion spectrum from precursor ion at *m/z* 230. (F) Product ion spectrum from precursor ion at *m/z* 228.

or $^{18}O_2$ atmosphere. The resulting 9,10-endoperoxides EAS^{16}O^{16}O and EAS^{18}O^{18}O were analyzed by HPLC-ESI-MS/MS (Fig. 6 and Supplementary Fig. 4 and 5). As expected in $^{16}O_2$ atmosphere, the endoperoxide EAS$^{16}O_2$ (MW 458) produced in the ezymatic reaction exhibits a $[M\text{-}2H]^{2-}$ ion at *m/z* 228 (Supplementary Fig. 5D). Only the SRM chromatogram of EAS$^{16}O_2$ with the mass transition *m/z* 228 to 212 can be detected at 7.9 min (Supplementary Fig. 5C). The SRM chromatogram showed no peaks for the EAS$^{18}O_2$ mass transition (*m/z* 230 to 212) (Supplementary Fig. 5B).

Conversely, when the HRP-catalyzed reaction was conducted under [^{18}O]-labeled dioxygen ($^{18}O_2$) enriched atmosphere, the fully labeled endoperoxide (EAS^{18}O^{18}O) appeared as the most abundant ion at *m/z* 230 (Fig. 6D). The ion corresponding to unlabeled endoperoxide (EAS^{16}O^{16}O) at *m/z* 228 was also detected with a relative abundance of about 50% compared to the fully labeled endoperoxide. Trace amounts of partially labeled endoperoxide (EAS^{18}O^{16}O) was also observed (Supplementary Fig. 4C). The detection of unlabeled and partially labeled endoperoxides can be attributed to residual oxygen ($^{16}O_2$) present in the reaction media after the freeze-thawing cycles to replace the dissolved $^{16}O_2$ with $^{18}O_2$.

Subsequently, the experiments were conducted in the presence of [^{18}O]-labeled O_2 ($^3\Sigma_g^-$). The EAS^{x}O$_2$ endoperoxides formed in the presence of the triplet ketone enzymatic generator systems show two intense $[M\text{-}2H]^{2-}$ ions at *m/z* 228 and 230 (Fig. 6D), corresponding to the molecular weights of 458 and 462 for the endoperoxides EAS^{16}O^{16}O and EAS^{18}O^{18}O, respectively. This is indicative of the incorporation of two 16- or 18- oxygen atoms into the anthracene endoperoxide molecules. The signal of the ion corresponding to the unlabeled anthracene endoperoxide at *m/z* 228 was detected with a relative abundance of 50% compared to that of the [^{18}O]-labeled oxygen anthracene endoperoxide molecule at *m/z* 230. The generation of traces of EAS^{18}O^{16}O (Supplementary Fig. 4C) and minor amounts of EAS$^{16}O_2$ was also observed in the EASO$_2$ MS spectrum, which can be attributed to residual $^{16}O_2$ contaminant after the freeze-thawing cycles to replace the dissolved $^{16}O_2$ with $^{18}O_2$ and to subdue the incidence of natural light during sample handling. Because the initial step of HRP-catalyzed IBAL oxidation involves the generation of an IBAL resonant α-hydroperoxyl/enolyl radical, which ultimately yields the 3-hydroxy-4,4-dimethyldioxetane intermediate – the putative precursor of triplet acetone and formic acid[65] by thermolysis, O_2 ($^1\Delta_g$) may have arisen from the radical, according to the Russell mechanism[16]. This route can be safely disregarded because TMD alone would not have been able to yield a consistent amount of EAS^{18}O^{16}O (Fig. 5) and the radical does not bear a geminal hydrogen, a necessary condition for singlet molecular oxygen generation by the Russell reaction[16]. Sulfur stable isotope distribution in EAS$^{16}O_2$ and EAS$^{18}O_2$ molecules was also observed by Ultra High Resolution MS, providing further confirmation of the EAS endoperoxide structures (Supplementary Fig. 6 and 7).

When the IBAL/HRP system was investigated under aerated condition (Supplementary Fig. 7), an analysis of the peak corresponding to *m/z* transition 228 to 212 indicated that 2.0 ± 0.4 μM O_2 ($^1\Delta_g$) is formed. A previous report stated that the HRP-catalyzed oxidation of IBAL generates at least 20% O_2 ($^1\Delta_g$)[65]. Much less optimistic, the yield of O_2 ($^1\Delta_g$) measured in our enzymatic experiments points to approximately 0.1%. Nevertheless, one must consider that the HRP-catalyzed reaction consumes the dissolved oxygen[65], thus gradually suppressing the generation of both triplet carbonyls and O_2 ($^1\Delta_g$).

Moreover, when the HRP/IBAL enzymatic reaction was conducted in the presence of 5 mM sorbate ion, a decrease in EASO$_2$ was observed (Supplementary Fig. 8). The EASO$_2$ EAS transition peak is 3-fold lower than the control peak (Supplementary Fig. 8B). Compared to the TMD chemiluminescence experiment in the presence of 0.5 mM sorbate (Supplementary Fig. 1A), the quenching

efficiency of 5 mM sorbate is lower in the generation of O_2 ($^1\Delta_g$) that accompanies the HRP-catalyzed oxidation of IBAL. This is predicted by the fact that the enzymatic system probably produces fewer triplet carbonyls than TMD and that the enzyme structure offers a collisional barrier for triplet acetone quenching produced in the active site[22]. Excited triplet acetone was estimated to be produced at a rate of 0.19 μM.min^{-1} by 10 mM IBAL in the presence of 5 μM HRP (Fig. 3). A noteworthy fact is that the decay of light emission parallels the oxygen consumption by the enzymatic reaction[66].

Discussion

It is well established that electronically excited triplet carbonyl products are produced chemically or enzymatically *via* the thermolysis of dioxetane intermediates[1,3,4,8].

Carbonyls in the triplet excited state are known to undergo unimolecular reactions (e.g., isomerization, α- and β-cleavage) and bimolecular processes (e.g., hydrogen abstraction, (2+2) cycloadditions), or to act as an electronic energy donor to a wide spectrum of biomolecules, thus triggering typically photochemical reactions. This inspired Cilento[10,67] and White[11], in the mid-1970s, to postulate independently that chemically or enzymatically generated triplet species in cells may drive physiological and/or pathological processes in the dark, a phenomenon they coined as "photochemistry and photobiology without light," or "photochemistry in the dark." The isomerization of natural products (e.g., colchicine, santonin), initiation of polyunsaturated fatty acid peroxidation, generation of the plant hormone ethylene, formation of cyclobutane thymine dimers, and several other biological processes, have been predicted and some of them have been shown to occur in the dark via triplet carbonyl intermediates[18].

Our results show for the first time that singlet molecular oxygen is produced enzymatically. This paper described the generation of O_2 ($^1\Delta_g$) via energy transfer from excited triplet acetone from both the thermolysis of TMD and the aerobic oxidation of HRP-catalyzed IBAL.

The chemiluminescent catalytic activity of hemeproteins such as cytochrome *c* acting on the peroxidation of fatty acids[24,29], and soybean lipoxygenase[68] or myeloperoxidase[69] inducing the oxidation of IBAL, were also accounted for by enzymatic sources of triplet excited species. The generation of methylglyoxal and diacetyl, putatively in the triplet state, by the oxidation of myoglobin-catalyzed aerobic oxidation of acetoacetate and 2-methylacetoacetate, respectively, was reported more recently[70].

From the biological viewpoint, it is worth mentioning that the generation of electronically excited triplet carbonyls in biological systems has been shown to cause oxidative injury to biologically important molecules such as DNA[71] and proteins, to trigger lipid peroxidation[72], and to induce phosphate-mediated permeabilization of isolated rat liver mitochondria[73].

In this work the formation of O_2 ($^1\Delta_g$) in chemical and enzymatic reactions was clearly demonstrated by direct detection of the O_2 ($^1\Delta_g$) monomol light emission at 1,270 nm using a photomultiplier coupled to a monochromator (Fig. 1C, 2B and 3B); and the observation of the effect of D_2O on the acquisition of the spectrum of the light emitted in the near infrared region showing an emission with maximum intensity at 1,270 nm (Fig. 1D).

Another evidence supporting the involvement of this mechanism was obtained by the direct detection of radicals TEMPO in the incubation reaction of TMD or HRP/IBAL with TEMP (Supplementary Fig. 2). The observed EPR spectrum suggests the presence of O_2 ($^1\Delta_g$) in the reaction mixture due to a mechanism involving energy transfer from the excited triplet acetone generated to molecular oxygen.

Finally the transfer mechanism involved in the generation of O_2 ($^1\Delta_g$) was studied using [^{18}O]-labeled molecular oxygen. Experiments conducted with $^{18}O_2$ in the presence of EAS (Fig. 4), showed that TMD thermolysis and the enzymatic HRP/IBAL generation of excited triplet acetone yields a mixture of endoperoxides containing ^{18}O and/or ^{16}O atoms namely EAS^{16}O^{16}O, EAS^{18}O^{18}O (Fig. 5 and 6 and Supplementary Fig. 3 to 7), EAS^{16}O^{18}O (Supplementary Fig. 4). Comparison of the relative amounts of EAS^{16}O^{16}O:EAS^{16}O^{18}O:EAS^{18}O^{18}O detected before and after removal of molecular oxygen showed a significant increase in the amount of EAS^{18}O^{18}O and a decrease in the amount of both EAS^{16}O^{16}O (Fig. 5 and 6). These results indicate that the reactions yield mainly $^{18}O_2$ ($^1\Delta_g$). The differences observed with and without [^{18}O]-labeled molecular oxygen shows that the ^{16}O-oxygen molecule present in the reaction mixture decreases the amount of detected $^{18}O_2$ ($^1\Delta_g$).

The decrease in the amount of $^{18}O_2$ ($^1\Delta_g$) detected in the presence of oxygen may be explained by an energy transfer mechanism between $^{18}O_2$ ($^1\Delta_g$) and $^{16}O_2$ ($^3\Sigma_g^-$), yielding $^{16}O_2$ ($^1\Delta_g$) and $^{18}O_2$ ($^3\Sigma_g^-$) as recently demonstrated for aqueous system by Martinez *et al.*[44].

The chemiluminescence, EPR and chemical trapping of $^{18}O_2$ ($^1\Delta_g$) experiments were also performed in the presence of sorbate, showing a triplet carbonyl quenching effect.

Quenching of triplet carbonyls by the addition of conjugated dienes such as hexa-2,4-dienoates (sorbates)[18] or even by the presence of ground state, triplet molecular oxygen can abate the level of chemical damage promoted by triplets to studied targets, either biomolecules or cell organelles[74,75].

Considering the enzymatic reactions that give rise to $^{18}O_2$ ($^1\Delta_g$) through a dioxetane intermediate involving a peroxyl radical. An alternative mechanism by which the formation of $^{18}O_2$ ($^1\Delta_g$) could be explained is the Russell mechanism[16]. This requires the generation of [^{18}O]-labeled IBAL peroxyl radicals that recombine to form a hypothetical tetraoxide intermediate, which then decomposes to generate O_2 ($^1\Delta_g$). However, this mechanism can be disregarded because it requires the presence of a geminal hydrogen in the IBAL-derived hydroperoxyl radical for the formation of O_2 ($^1\Delta_g$) and the detection of O_2 ($^1\Delta_g$) containing a mixture of ^{16}O and ^{18}O atoms.

Conclusion

The present study unequivocally demonstrates that singlet molecular oxygen is generated by energy transfer from chemically and enzymatically produced excited triplet acetone to ground state triplet molecular oxygen in aqueous solution (Fig. 7).

This was substantiated by ultraweak CL studies in the near IR region at 1,270 nm with both chemical and enzymatic sources of triplet acetone, which is characteristic of the singlet delta state monomolecular decay of excited molecular oxygen. Indirect analysis based on mass spectrometry and EPR measurements strongly supports the formation of O_2($^1\Delta_g$). Moreover, the use of [^{18}O]-labeled molecular oxygen in association with HPLC-ESI-MS/MS analysis is a highly suitable way to gain relevant mechanistic insights into the formation of singlet molecular oxygen and the decomposition pathways of initially generated peroxide compounds such as dioxetanes and subsequently excited ketones.

The quantum yield of singlet molecular oxygen was found to be higher in aqueous medium than previously demonstrated in organic solvents. This work proposes that enzymatically generated triplet carbonyl may be a contributing source of O_2 ($^1\Delta_g$) in non-illuminated biological systems such as root and liver tissues, as earlier proposed independently by Cilento[10] and White[11].

Biological implication - Taking into consideration that (i) molecular oxygen is *c.a.* ten times more soluble in membranes that in aqueous medium, (ii) membrane peroxidation involves the intermediacy of alkoxyl and alkylperoxyl radicals derived from polyunsaturated fatty acids, whose dismutation affords triplet carbonyls[18], and (iii) phosphate-induced and sorbate-inhibited deleterious permeabilization of mitochondrial membranes via amplification of triplet pro-

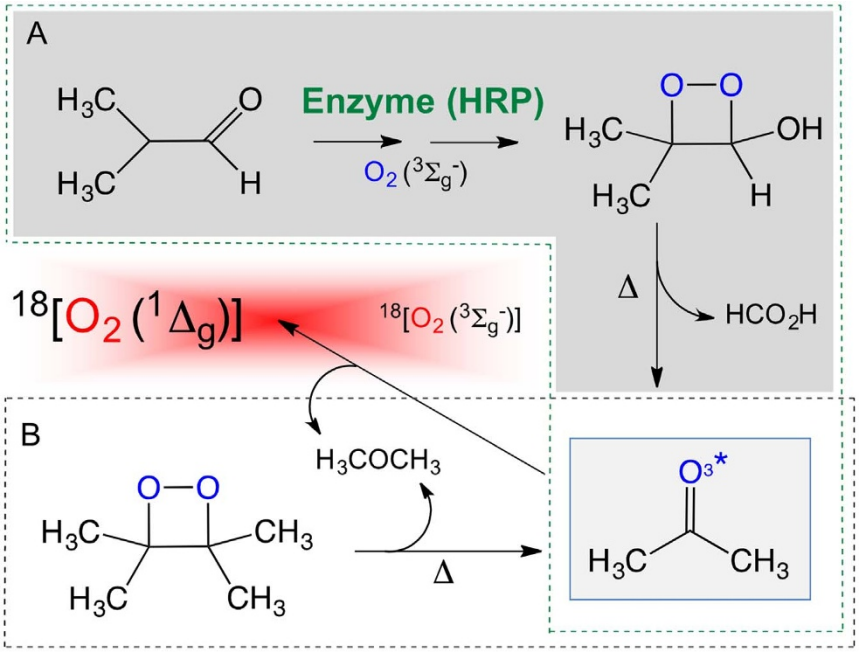

Figure 7 | Singlet molecular oxygen generated enzymatically (A) and chemically (B).

ducts[73], it is of utmost interest to investigate the participation of singlet molecular oxygen in membrane damage induced by pro-oxidants. In addition, membrane cholesterol and proteins could also be victimized by singlet molecular oxygen formed from triplet carbonyls leading to loss or gain of biological functions. In this regard, noteworthy are the findings by several groups[76–78] that cholesterol secoaldehyde formed by addition of ozone or singlet molecular oxygen to cholesterol may be implicated in atherosclerosis, Alzheimer disease, and apoptosis involving signaling pathways.

Methods

Materials Used. Peroxidase from horseradish (HRP) type VI, K_2HPO_4, KH_2PO_4, NH_4HCO_3, 2,2,6,6-tetramethylpiperidine (TEMP), 2,2,6,6-tetramethylpiperidine-1-oxyl (TEMPO) and hexa-2,4-dienoic acid (sorbic acid) were purchased from Sigma (St. Louis, MO). 2-Methylpropanal (isobutyraldehyde or isobutanal, IBAL), D_2O and CCl_4 were purchased from Aldrich (Steinheim, Germany). HPLC grade solvents were acquired from Merck (Darmstadt, Germany). IBAL was distilled before use. Deuterated phosphate buffer at pD 7.4 (equivalent to pH 7.0) was prepared by mixing D_2O stock solutions of KH_2PO_4 and K_2HPO_4. 3,3,4,4-Tetramethyl-1,2-dioxetane (TMD) was prepared as previously described by Kopecky et al.[57,58]. Standard anthracene-9,10-diyldiethane-2,1-diyl disulfate disodium salt (EAS) endoperoxide ($EASO_2$) was prepared by methylene blue photosensitization in aerated deuterium water containing 8 mM EAS, and was subsequently quantified spectrophotometrically[30,34,35,44,45]. 1,4-Dimethylnaphthalene (DMN) endoperoxide ($DMNO_2$) was also prepared by UVA irradiation of DMN/methylene blue and then quantified spectrophotometrically[60].

Low level luminescence emission of excited triplet acetone produced by thermal cleavage of TMD or oxidation of IBAL by HRP/H_2O_2 and NIR detection of the monomol light emission of O_2 ($^1\Delta_g$). TMD dissolved in CCl_4 at concentrations ranging from 2 to 10 mM was transferred from ice to a cuvette holder set at a temperature of 70°C. The light emission was immediately recorded by a FLSP 920 photon counter (Edinburgh Instruments, Edinburgh, UK) consisting of two UV-Visible Hamamatsu detectors R9110, maintained at −20°C by a CO1 thermoelectric cooler also purchased from Edinburgh Instruments. The detector used to measure the steady-state light emission from TMD thermal cleavage was not preceded by any monochromator; therefore, light was recorded directly from the cuvette source. To trace the TMD-elicited chemiluminescence, a second detector was used and its wavelength was determined using a monochromator[35]. The chemical yield of 10 mM TMD-generated triplet acetone was confirmed in acetonitrile, reportedly evaluated as approximately 30%[58]. During each experiment, the monomol light emission of O_2 ($^1\Delta_g$) at 1,270 nm was monitored using the third detector coupled to the device, a Hamamatsu H10330A-45 apparatus (Hamamatsu city, Japan), also preceded by a monochromator. To determine the O_2 ($^1\Delta_g$) generation rate, 2 mM $DMNO_2$ in CCl_4 was used as the standard[29,33–35,60]. The same procedure was applied in the quenching studies of triplet acetone with different concentrations of sodium sorbate[18]. CL arising from the thermal decomposition of 10 mM TMD at 70°C was performed in acetonitrile or air-equilibrated CCl_4. The CL spectrum of the triplet excited acetone was obtained from 10 mM TMD in CCl_4 at 70°C. The same equipment and procedure were used to observe the generation of triplet excited acetone produced during 5 μM HRP-catalyzed oxidation of 10 mM IBAL and 0.10 mM H_2O_2 in deuterated aqueous 50 mM phosphate buffer (pD 7.4) at 37°C.

The NIR spectrum of O_2 ($^1\Delta_g$) at 1,270 nm was produced by thermal decomposition of 1,4-dimethylnaphthalene endoperoxide ($DMNO_2$) at 50°C[60].

EPR spin-trapping studies with TEMP. Samples containing 50 mM TEMP[64] and 4 mM TMD were prepared in phosphate buffer (pH 7.4) and incubated for 4 min at 60°C. The reacting solutions were then transferred to an appropriate cuvette and the EPR spectra recorded in an EMX spectrometer (Bruker, Silberstreifen, Germany), using the following parameters: frequency: 100.0 kHz; amplitude: 0.5 mT; time constant 81.920 ms; time conversion: 40.960 ms; and gain: 2.52×10^4.

The experiment with enzymatically generated triplet acetone were conducted in 50 mM phosphate buffer (pH 7.4) that contained 20 μM HRP, 100 mM IBAL and 50 mM TEMP, incubated for 6 min at 37°C and immediately transferred to the cuvette. The EPR parameters used were the same as for TMD, both in the absence and presence of 8 mM sorbate, a triplet acetone quencher. In order to confirm the attribution of the EPR signal to the reaction product of TEMP treated with O_2 ($^1\Delta_g$), the spectrum was spiked by addition of 0.4 μM TEMPO to the solution. Computational simulations of the EPR signals were performed using the Winsin program[79].

Chemical trapping of O_2 ($^1\Delta_g$) by EAS and [^{18}O]-labeled experiments. To unequivocally attest singlet molecular oxygen 9,10-cycloaddition to the EAS probe yielding $EASO_2$, a sample containing 8 mM TMD and 8 mM EAS was prepared in $^{18}O_2$-purged solutions as follows. TMD/EAS samples were transferred to a closed system and degassed by three freeze-thaw cycles using a vacuum pump. The degassed solution was saturated with $^{18}O_2$ for 2 h and heated at 70°C. The same procedure was employed as above but without dearating the solution. These samples were kept at 70°C using a Termomixer (Eppendorf, City, Germany) for 24 h.

The degassing-saturation procedure using argon gas was applied to prepare the reaction mixture containing 8 mM EAS, 5 μM HRP, 0.1 mM H_2O_2 and 50 mM IBAL, except that it was kept in the dark under room temperature for 72 h. Quantification of $EAS^{18}O_2$ using the HRP/IBAL system was carried out under similar concentration conditions, but the reacting solutions were kept under continuous stirring using a Termomixer apparatus (Hamburg, Germany) for 24 h at 37°C.

HPLC-ESI-MS/MS detection of $EASO_2$. HPLC-ESI-MS/MS analyses of the anthracene endoperoxide $EASO_2$ were conducted by injecting 25 μL of the sample in a Shimadzu HPLC system (Tokyo, Japan) coupled to a mass spectrometer Quattro II triple quadrupole (Micromass, Manchester, UK). Endoperoxide $EASO_2$ was separated using a Luna C18 reverse phase column, 250 × 4.6 mm, 5 μM particle size (Phenomenex, Torance, CA,) that was kept at 25°C. The liquid phase consisted of

25 mM ammonium formate (solvent A) and acetonitrile:methanol 7 : 3, v/v (solvent B) with linear gradient of 25% B during 15 min, 25 to 70% B for 1 min, 70% B until 25 min, 70 to 25% B during 1 min and 25% B until 30 min. The eluent was monitored at 210 nm with a flow rate of 0.8 mL.min^{-1}. First 5 min of run gradient was discarded and 10% of flow rate was directed to the mass spectrometer. Ionization of the sample was obtained by electrospray ion source (ESI) in the negative ion mode using the following parameters: source temperature, 120°C; desolvation temperature, 200°C; cone voltage, 15 V; collision energy, 10 eV. The endoperoxides EAS^{x}O^{x}O were detected by the loss of the oxygen molecule, in the Selected Reaction Monitoring mode (SRM). The transitions recorded were *m/z* 228→212 for EAS^{16}O^{16}O, *m/z* 229→212 for EAS^{18}O^{16}O and *m/z* 230→212 for EAS^{18}O^{18}O.

UHR-ESI-Q-TOF detection of EASO$_2$. High resolution mass spectrometry analysis of EAS^{x}O^{x}O endoperoxides were performed in an UHPLC Agilent coupled to an UHR-ESI-Q-TOF Bruker Daltonics MaXis 3G mass spectrometer with CaptiveSpray source in the negative mode. The UHPLC mobile phase consisted of ammonium formate (solvent A) and acetonitrile:methanol 7 : 3, v/v (solvent B) with the following linear gradient: 25% B during 15 min, 25 to 70% B for 1 min, 70% B until 25 min, 70 to 25% B during 1 min and 25% B until 30 min. Endoperoxides was separated on a Luna C18 reverse phase column, 250 × 4.6 mm, 5 µM particle size (Phenomenex, Torance, CA) and monitored at 210 nm. The flow rate was 0.8 mL.min^{-1}. Reverse phase column was kept at 30°C. The ESI conditions were: capillary, 4.0 kV; dry heater, 180 °C; dry gas, 8.0 l/min; end plate, −450 V. Nitrogen was used as collision gas and the CID (collision-induced dissociation) energy was 10 eV. The instrument was externally calibrated using an ESI low concentration tuning mix over the m/z range of 100 to 2000. The Bruker Data Analysis software (version 4.0) was employed for data acquisition and processing.

1. Cilento, G. [Electronic excitation in dark biological processes]. *Chemical and Biological Generation of Excited States.* [Adam, W. & Cilento, G. (eds.)] [277–307] (Academic Press, New York, 1982).
2. Frimer, A. A. (ed.) *Singlet Oxygen* [Vol. I–IV] (CRC Press, Boca Raton, 1985).
3. Murphy, M. E. & Sies, H. Visible-range low-level chemiluminescence in biological systems. *Meth. Enzymol.* **186**, 595–610 (1990).
4. Sies, H. (ed.) *Oxidative Stress, Oxidants and Antioxidants*. (Academic Press, Orlando 1991).
5. Cadet, J. & Di Mascio, P. [Peroxide in biological systems]. *The Chemistry of Peroxides.* [Rappoport, Z. (ed.)] [915–999] (Wiley, Chichester, 2006).
6. Sugioka, K. & Nakano, M. Possible mechanism of generation of singlet molecular-oxygen in NADPH-dependent microsomal lipid peroxidation. *Biochim. Biophys. Acta* **423**, 203–216 (1976).
7. Cadenas, E. Lipid-peroxidation during the oxidation of hemoproteins by hydroperoxides - relation to electronically excited-state formation. *J. Biolumin. Chemilum.* **4**, 208–218 (1989).
8. Adam, W., Reinhardt, D. & Saha-Möller, C. R. From the firefly bioluminescence to the dioxetane-based (AMPPD) chemiluminescence immunoassay: A retroanalysis. *Analyst* **121**, 1527–1531 (1996).
9. Viviani, V. R. & Bechara, E. J. H. Bioluminescence of Brazilian fireflies (Coleoptera, Lampyridae) - Spectral distribution and pH effect on luciferase-elicited colors - Comparison with elaterid and phengodid luciferases. *Photochem. Photobiol.* **62**, 490–495 (1995).
10. Cilento, G. Excited electronic states in dark biological process. *Q. Rev. Biophys.* **6**, 485–501 (1973).
11. White, E. H. & Wei, C. C. A possible role for chemically-produced excited states in biology. *Biochem. Biophys. Res. Commun.* **39**, 1219–1223 (1970).
12. Mendenhall, G. D., Sheng, X. C. & Wilson, T. Yields of excited carbonyl species from alkoxyl and from alkylperoxyl radical dismutations. *J. Am. Chem. Soc.* **113**, 8976–8977 (1991).
13. Bechara, E. J. H., Baumstark, A. L. & Wilson, T. Tetraethyldioxetane and 3,4-dimethyl-3,4-di-n-butyl-1,2-dioxetane. High ratio of triplet to singlet excited products from the thermolysis of both dioxetanes. *J. Am. Chem. Soc.* **98**, 4648–4649 (1976).
14. Adam, W. & Baader, W. J. Effects of methylation on the thermal-stability and chemiluminescence properties of 1,2-dioxetanes. *J. Am. Chem. Soc.* **107**, 410–416 (1985).
15. Farneth, W. E. & Johnson, D. G. Chemi-luminescence in the infrared photochemistry of oxetanes - the formal reverse of ketone photocycloaddition. *J. Am. Chem. Soc.* **106**, 1875–1876 (1984).
16. Russell, G. A. Deuterium-isotope effects in the autoxidation of aralkyl hydrocarbons. Mechanism of the interaction of peroxy radicals. *J. Am. Chem. Soc.* **79**, 3871–3877 (1957).
17. Miyamoto, S., Martinez, G. R., Medeiros, M. H. G. & Di Mascio, P. Singlet molecular oxygen generated from lipid hydroperoxides by the Russell mechanism: Studies using O-18-labeled linoleic acid hydroperoxide and monomol light emission measurements. *J. Am. Chem. Soc.* **125**, 6172–6179 (2003).
18. Velosa, A. C., Baader, W. J., Stevani, C. V., Mano, C. M. & Bechara, E. J. H. 1,3-Diene probes for detection of triplet carbonyls in biological systems. *Chem. Res. Toxicol.* **20**, 1162–1169 (2007).
19. Noll, T., deGroot, H. & Sies, H. Distinct temporal relation among oxygen-uptake, malondialdehyde formation, and low-level chemiluminescence during microsomal lipid-peroxidation. *Arch. Biochem. Biophys.* **252**, 284–291 (1987).
20. Timmins, G. S. *et al.* Lipid peroxidation-dependent chemiluminescence from the cyclization of alkylperoxyl radicals to dioxetane radical intermediates. *Chem. Res. Toxicol.* **10**, 1090–1096 (1997).
21. Di Mascio, P., Catalani, L. H. & Bechara, E. J. H. Are dioxetanes chemiluminescent intermediates in lipoperoxidation? *Free Radic. Biol. Med.* **12**, 471–478 (1992).
22. Bechara, E. J. H., Oliveira, O. M. M. F., Duran, N., de Baptista, R. C. & Cilento, G. Peroxidase catalyzed generation of triplet acetone. *Photochem. Photobiol.* **30**, 101–110 (1979).
23. Cilento, G. Generation of triplet carbonyl-compounds during peroxidase catalyzed-reactions. *J. Biolumin. Chemilumin.* **4**, 193–199 (1989).
24. Cadenas, E., Boveris, A. & Chance, B. Chemi-luminescence of lipid vesicles supplemented with cytochrome-c and hydroperoxide. *Biochem. J.* **188**, 577–583 (1980).
25. Foote, C. S. & Denny, R. W. Chemistry of singlet oxygen. Quenching by beta-carotene. *J. Am. Chem. Soc.* **90**, 6233–& (1968).
26. Abdel-Shafi, A. A., Worrall, D. R. & Wilkinson, F. Singlet oxygen formation efficiencies following quenching of excited singlet and triplet states of aromatic hydrocarbons by molecular oxygen. *J. Photochem. Photobiol. A* **142**, 133–143 (2001).
27. Briviba, K., Saha-Möller, C. R., Adam, W. & Sies, H. Formation of singlet oxygen in the thermal decomposition of 3-hydroxymethyl-3,4,4-trimethyl-1,2-dioxetane, a chemical source of triplet-excited ketones. *Biochem. Mol. Biol. Int.* **38**, 647–651 (1996).
28. Frimer, A. A. Reaction of singlet oxygen with olefins - Question of mechanism. *Chem. Rev.* **79**, 359–387 (1979).
29. Miyamoto, S. *et al.* Cytochrome c-promoted cardiolipin oxidation generates singlet molecular oxygen. *Photochem. Photobiol. Sci.* **11**, 1536–1546 (2012).
30. Miyamoto, S. *et al.* Linoleic acid hydroperoxide reacts with hypochlorous acid, generating peroxyl radical intermediates and singlet molecular oxygen. *Proc. Natl. Acad. Sci.USA* **103**, 293–298 (2006).
31. Bechara, E. J. H. & Wilson, T. Alkyl substituent effects on dioxetane properties. Tetraethyl-, dicyclohexylidene-, and 3,4-dimethyl-3,4-di-n-butyldioxetanes. A discussion of decomposition mechanisms. *J. Org. Chem.* **45**, 5261–5268 (1980).
32. Kanofsky, J. R. & Sima, P. Singlet oxygen production from the reactions of ozone with biological molecules. *J. Biol. Chem.* **266**, 9039–9042 (1991).
33. Di Mascio, P., Bechara, E. J. H., Medeiros, M. H. G., Briviba, K. & Sies, H. Singlet molecular oxygen production in the reaction of peroxynitrite with hydrogen peroxide. *FEBS Lett.* **355**, 287–289 (1994).
34. Martinez, G. R. *et al.* Peroxynitrite does not decompose to singlet oxygen ($^1\Delta_gO_2$) and nitroxyl (NO^-). *Proc. Natl. Acad. Sci. USA* **97**, 10307–10312 (2000).
35. Miyamoto, S. *et al.* Direct evidence of singlet molecular oxygen generation from peroxynitrate, a decomposition product of peroxynitrite. *Dalton Trans.* **29**, 5720–5729 (2009).
36. Moureu, C., Dufraisse, C. & Dean, P. M. An organic peroxide separable from the rubrene peroxide. *C. R. Hebd. Seances Acad. Sci.* **182**, 1584–1587 (1926).
37. Dufraisse, C. & Velluz, L. The labile union of carbon and peroxide which spontaneously dissociates in the cold. *C. R. Hebd. Seances Acad. Sci.* **208**, 1822–1824 (1939).
38. Wasserman, H. H. & Larsen, D. L. Formation of 1,4-endoperoxides from dye-sensitized photooxygenation of alkyl-naphthalenes. *J. Chem. Soc. Chem. Comm.* **5**, 253–254 (1972).
39. Di Mascio, P. & Sies, H. Quantification of singlet oxygen generated by thermolysis of 3,3'-(1,4-naphthylene)dipropionate endoperoxide. Monomol and dimol photoemission and the effects of 1,4-diazabicyclo[2.2.2]octane. *J. Am. Chem. Soc.* **111**, 2909–2914 (1989).
40. Pierlot, C., Aubry, J. M., Briviba, K., Sies, H. & Di Mascio, P. Naphthalene endoperoxides as generators of singlet oxygen in biological media. *Meth. Enzymol.* **319**, 3–20 (2000).
41. Saito, I., Matsuura, T. & Inoue, K. Formation of superoxide ion from singlet oxygen - on the use of a water-soluble singlet oxygen source. *J. Am. Chem. Soc.* **103**, 188–190 (1981).
42. Ravanat, J.-L., Di Mascio, P., Martinez, G. R., Medeiros, M. H. G. & Cadet, J. Singlet oxygen induces oxidation of cellular DNA. *J. Biol. Chem.* **275**, 40601–40604 (2000).
43. Ravanat, J.-L. *et al.* Singlet oxygen-mediated damage to cellular DNA determined by the comet assay associated with DNA repair enzymes. *Biol. Chem.* **385**, 17–20 (2005).
44. Martinez, G. R. *et al.* Energy transfer between singlet ($^1\Delta_g$) and triplet ($^3\Sigma_g^-$) molecular oxygen in aqueous solution. *J. Am. Chem. Soc.* **126**, 3056–3057 (2004).
45. Martinez, G. R., Ravanat, J.-L., Medeiros, M. H. G., Cadet, J. & Di Mascio, P. Synthesis of a naphthalene endoperoxide as a source of ^{18}O-labeled singlet oxygen for mechanistic studies. *J. Am. Chem. Soc.* **122**, 10212–10213 (2000).
46. Rolim, J. P. M. L. *et al.* The antimicrobial activity of photodynamic therapy against *Streptococcus mutans* using different photosensitizers. *J. Photochem. Photobiol. B* **106**, 40–46 (2012).
47. Yoon, H. Y. *et al.* Tumor-targeting hyaluronic acid nanoparticles for photodynamic imaging and therapy. *Biomaterials* **33**, 3980–3989 (2012).

48. Baumler, W., Regensburger, J., Knak, A., Felgentrager, A. & Maisch, T. UVA and endogenous photosensitizers - the detection of singlet oxygen by its luminescence. *Photochem. Photobiol. Sci.* **11**, 107–117 (2012).
49. Henderson, B. W. & Dougherty, T. J. How does photodynamic therapy work. *Photochem. Photobiol.* **55**, 145–157 (1992).
50. Chin, K. K. *et al.* Quantitative determination of singlet oxygen generated by excited state aromatic amino acids, proteins, and immunoglobulins. *J. Am. Chem. Soc.* **130**, 6912–6913 (2008).
51. Prado, F. M. *et al.* Thymine hydroperoxide as a potential source of singlet molecular oxygen in DNA. *Free Radic. Biol. Med.* **47**, 401–409 (2009).
52. Krinsky, N. I. Singlet excited oxygen as a mediator of antibacterial action of leukocytes. *Science* **186**, 363–365 (1974).
53. Steinbeck, M. J., Khan, A. U. & Karnovsky, M. J. Intracellular singlet oxygen generation by phagocytosing neutrophils in response to particles coated with a chemical trap. *J. Biol. Chem.* **267**, 13425–13433 (1992).
54. Steinbeck, M. J., Khan, A. U. & Karnovsky, M. J. Extracellular production of singlet oxygen by stimulated macrophages quantified using 9,10-diphenylanthracene and perylene in a polystyrene film. *J. Biol. Chem.* **268**, 15649–15654 (1993).
55. Cadet, J., Ravanat, J.-L., Martinez, G. R., Medeiros, M. H. G. & Di Mascio, P. Singlet oxygen oxidation of isolated and cellular DNA: Product formation and mechanistic insights. *Photochem. Photobiol.* **82**, 1219–1225 (2006).
56. Müller-Breitkreutz, K., Mohr, H., Briviba, K. & Sies, H. Inactivation of viruses in human plasma by singlet molecular oxygen. *J. Photochem. Photobiol. B.* **30**, 63–70 (1995).
57. Kopecky, K. R., Filby, J. E., Mumford, C., Lockwood, P. A. & Ding, J. Y. Preparation and thermolysis of some 1,2-dioxetanes. *Can. J. Chem.* **53**, 1103–1122 (1975).
58. Turro, N. J. & Lechtken, P. Molecular photochemistry. LII. Thermal-decomposition of tetramethyl-1,2-dioxetane. Selective and efficient chemelectronic generation of triplet acetone. *J. Am. Chem. Soc.* **94**, 2886–2888 (1972).
59. Krinsky, N. I. Singlet oxygen in biological-systems. *Trends Biochem. Sci.* **2**, 35–38 (1977).
60. Di Mascio, P., Bechara, E. J. H. & Rubim, J. C. Dioxygen NIR FT-emission ($^1\Delta_g \rightarrow {}^3\Sigma^-_g$) and Raman spectra of 1,4-dimethylnaphthalene endoperoxide: A source of singlet molecular-oxygen. *Appl. Spectrosc.* **46**, 236–239 (1992).
61. Mcgarvey, D. J., Szekeres, P. G. & Wilkinson, F. The efficiency of singlet oxygen generation by substituted naphthalenes in benzene - Evidence for the participation of charge-transfer interactions. *Chem. Phys. Lett.* **199**, 314–319 (1992).
62. Wilkinson, F., Helman, W. P. & Ross, A. B. Rate constants for the decay and reactions of the lowest electronically excited singlet-state of molecular-oxygen in solution - an expanded and revised compilation. *J. Phys. Chem. Ref. Data.* **24**, 663–1021 (1995).
63. Di Mascio, P., Kaiser, S. & Sies, H. Lycopene as the most efficient biological carotenoid singlet oxygen quencher. *Arch. Biochem. Biophys.* **274**, 532–538 (1989).
64. Lavi, R. *et al.* ESR detection of $^1O_2$ reveals enhanced redox activity in illuminated cell cultures. *Free Radic. Res.* **38**, 893–902 (2004).
65. Cilento, G. Generation of electronically excited triplet species in biochemical systems. *Pure Appl. Chem.* **56**, 1179–1190 (1984).
66. Baader, W. J., Bohne, C., Cilento, G. & Dunford, H. B. Peroxidase-catalyzed formation of triplet acetone and chemiluminescence from isobutyraldehyde and molecular oxygen. *J. Biol. Chem.* **260**, 10217–10225 (1985).
67. Cilento, G. Dioxetanes as intermediates in biological processes. *J. Theor. Biol.* **55**, 471–479 (1975).
68. Schulte-Herbrüggen, T. & Sies, H. The peroxidase oxidase activity of soybean lipoxygenase. Triplet excited carbonyls from the reaction with isobutanal and the effect of glutathione. *Photochem. Photobiol.* **49**, 697–704 (1989).
69. Nascimento, A. L., da Fonseca, L. M., Brunetti, I. L. & Cilento, G. Intracellular generation of electronically excited states. Polymorphonuclear leukocytes challenged with a precursor of triplet acetone. *Biochim. Biophys. Acta* **881**, 337–342 (1986).
70. Ganini, D. *et al.* Myoglobin-H_2O_2 catalyzes the oxidation of β-ketoacids to α-dicarbonyls: mechanism and implications in ketosis. *Free Radic. Biol. Med.* **51**, 733–743 (2011).
71. Adam, W. *et al.* Photobiological studies with dioxetanes in isolated DNA, bacteria, and mammalian-cells. *Environ. Health Perspect.* **88**, 89–97 (1990).
72. Almeida, A. M., Bechara, E. J. H., Vercesi, A. E. & Nantes, I. L. Diphenylacetaldehyde-generated excited states promote damage to isolated rat liver mitochondrial DNA, phospholipids, and proteins. *Free Radic. Biol. Med.* **27**, 744–751 (1999).
73. Kowaltowski, A. J., Castilho, R. F., Grijalba, M. T., Bechara, E. J. H. & Vercesi, A. E. Effect of inorganic phosphate concentration on the nature of inner mitochondrial membrane alterations mediated by Ca^{2+} ions - A proposed model for phosphate-stimulated lipid peroxidation. *J. Biol. Chem.* **271**, 2929–2934 (1996).
74. Augusto, O. & Bechara, E. J. H. Hemin-catalyzed generation of triplet acetone. *Biochim. Biophys. Acta* **631**, 203–209 (1980).
75. Darmanyan, A. P. & Foote, C. S. Solvent effects on singlet oxygen yield from nπ* and ππ* triplet carbonyl-compounds. *J. Phys. Chem.* **97**, 5032–5035 (1993).
76. Wentworth, P. Jr. *et al* Evidence for ozone formation in human atherosclerotic arteries. *Science* **302**, 1053–1056 (2003).
77. Uemi, M. *et al.* Generation of cholesterol carboxyaldehyde by the reaction of singlet molecular oxygen [O_2 ($^1\Delta_g$)] as well as ozone with cholesterol. *Chem. Res. Toxicol.* **22**, 875–884 (2009).
78. Laynes, L., Raghavamenon, A. C., D'Auvergne, O. & Achuthan, V. Uppu RM MAPK signaling in H9c2 cardiomyoblasts exposed to cholesterol secoaldehyde--role of hydrogen peroxide. *Biochem. Biophys. Res. Commun.* **404**, 90–95 (2011).
79. Duling, D. R. Simulation of multiple isotropic spin-trap EPR-spectra. *J. Magn. Reson. B* **104**, 105–110 (1994).

Acknowledgments

This work is dedicated *in memoriam* to Giuseppe Cilento (University of São Paulo) and Emil H. White (Johns Hopkins University), who independently postulated the hypothesis of "photo(bio)chemistry in the dark" to explain the occurrence of "photoproducts" in animal and vegetal tissues hidden from light. We thank I. L. Nantes for reading the manuscript. We are also indebted to Dr. Ohara Augusto for the EPR facility. The authors acknowledge the financial support of the Brazilian research funding institutions FAPESP (Fundação de Amparo à Pesquisa do Estado de São Paulo; No. 2006/56530-4 and No. 2012/12663-1), CNPq (Conselho Nacional para o Desenvolvimento Científico e Tecnológico), CAPES (Coordenação de Aperfeiçoamento de Pessoal de Nível Superior), PRONEX/FINEP (Programa de Apoio aos Núcleos de Excelência), PRPUSP (Pro-Reitoria de Pesquisa da Universidade de São Paulo), Instituto do Milênio-Redoxoma (No. 420011/2005-6), INCT Redoxoma (FAPESP/CNPq/CAPES; No. 573530/2008-4), NAP Redoxoma (PRPUSP; No. 2011.1.9352.1.8), CEPID Redoxoma (FAPESP; No. 2013/07937-8), Fundo Bunka de Pesquisa Banco Sumitomo Mitsui (fellowship granted to S. Miyamoto), L'OREAL (fellowships granted to G.R. Martinez and S. Miyamoto) and the John Simon Guggenheim Memorial Foundation (fellowships granted to P. Di Mascio and E.J.H. Bechara). H. Sies is a Fellow of the National Foundation for Cancer Research, Bethesda, MD, USA.

Author contributions

C.M.M., E.J.H.B., F.M.P. & P.D.M. contributed equally to this work. P.D.M., E.J.H.B., S.M., G.R.M., G.E.R., J.C., H.S. & M.H.G.M. developed the concept of the experiments and the analyses. P.D.M., F.M.P., C.M.M. & J.M. conducted the experiments. All the authors made significant contributions to the discussion and writing of this manuscript.

Additional information

Supplementary information accompanies this paper at http://www.nature.com/scientificreports

Competing financial interests: The authors declare no competing financial interests.

How to cite this article: Mano, C.M. *et al.* Excited singlet molecular O_2 ($^1\Delta_g$) is generated enzymatically from excited carbonyls in the dark. *Sci. Rep.* **4**, 5938; DOI:10.1038/srep05938 (2014).